

248 nm excimer laser drilling PI film for nozzle plate application

C. T. Pan · H. Yang · M. K. Wei

Received: 17 January 2006 / Accepted: 5 May 2006 / Published online: 15 June 2006
© Springer-Verlag London Limited 2006

Abstract In this study, drilling of polyimide (PI) film by using a 248 nm excimer laser through photomask projection is presented. The parameter effects of laser fluence, shot number and repetition rate on the processing results are realized. A high-quality of microhole array with 50 μm thick PI film has been fabricated. When the projection process is carried out, differences in the diameters of the microhole in the front and back sides of the PI are observed, which cause a conical shape in the kerf. The formation of this conical shape in terms of laser process parameters is discussed. Besides, to improve the laser machining quality of PI microholes, the effects of the process parameters are investigated and characterized. In addition, before excimer laser drilling PI is conducted, the PI surface is pre-coated with, or left without, a thin film material to observe the formation of debris. The results shows that the formation of debris can be reduced significantly when a pre-coated thin film is applied on the PI surface.

Keywords 248 nm excimer laser · Microholes · Nozzle plate · PI

1 Introduction

Micro-electro-mechanical system (MEMS) technology offers a wide variety of applications for the military, industrial, and biotechnology industries. Numerous academics and research institutions make efforts in the development of MEMS technology and commercial products [1]. The technology allows compact and mini-feature components to be fabricated. Micromachining with laser pulses is interesting, leading to the fabrication of microsystems and semiconductor devices. Due to the progress in the development of ultra-short lasers, for example, the excimer laser, the high flexibility of pattern generation can be combined with high resolution, high precision and high efficiency.

Much research on excimer laser micromachining of different kinds of materials with laser pulse has been published [2–6]. Most of the results reported only on the single microhole drilling process with diameters between 10 and 100 μm , but not in arrays. Microstructure is fabricated using an excimer laser because of its short wavelength [7–9]. Laser machining from near infrared (1064 nm) to ultraviolet (UV; 248 nm) was used for precision machining of materials in the micrometer range [10, 11]. Patterns on polymers, ceramics, and superconductors ablated by excimer lasers caused structures with less material damage [12]. Polymeric materials are suitable for microstructure due to their low ablation threshold, smooth etching behaviour, and ablation rates at tenths of micrometers per pulse at very modest energy fluence [13, 14]. Miniature devices with microholes can revolutionize many electro-mechanical-optical systems, such as micronozzle,

C. T. Pan
Department of Mechanical and Electro-Mechanical Engineering,
and Center for Nanoscience & Nanotechnology,
National Sun Yat-Sen University,
Kaoshiung 804, Taiwan

H. Yang (✉)
Institute of Precision Engineering,
National Chung Hsing University,
250 Kuo-Kuang Road,
Taichung 40227, Taiwan
e-mail: hsihamg@nchu.edu.tw

M. K. Wei
Department of Materials Science & Engineering,
National Dong Hwa University,
Hualien, Taiwan

ink jet nozzle [15], microchannels [16], biochips and microfluidic system-on-chip [17]. The fabrication of micro-hole array with both higher accuracy and lower cost is needed to match the rapid demand for these commercial devices. Material processing with excimer lasers is going to become an established technique for micromachining.

Drilling is one of the most common machining operations, and has been reported to account for up to 50% of all machining nationwide in the USA [18]. Various laser

technologies including UV laser, CO₂ laser, and Nd:YAG lasers have been selected for printed circuit board (PCB) application. There are many problems for UV laser drilling. One of the most important issues is that aspect ratio of obtained holes (i.e. the ratio of a hole depth to its diameter) is usually not high. The effect of plasma confinement on material ablation has been investigated [19]. The CO₂ laser emits light in the infrared (10.6 μm) where absorption in dielectric materials is more than 90%. The absorption depth

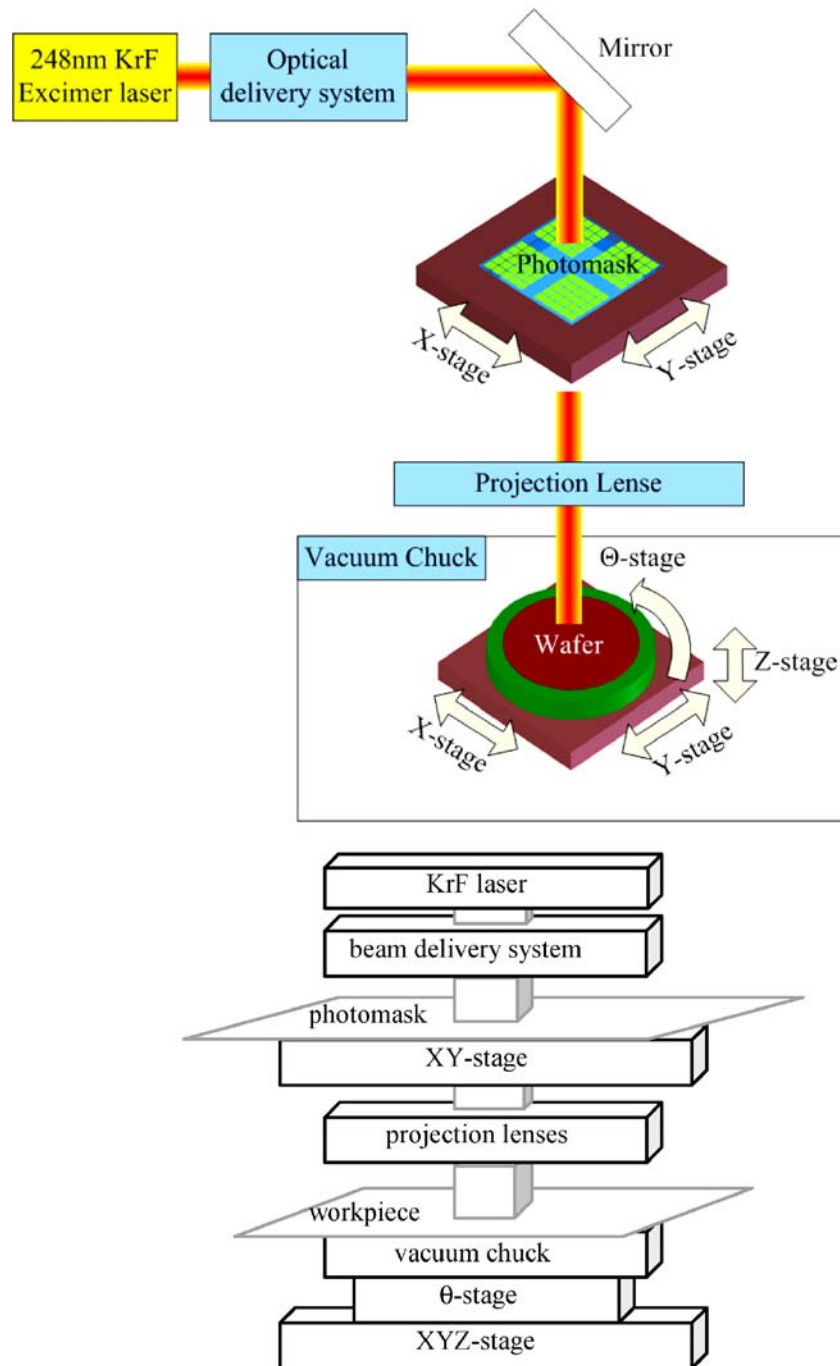


Fig. 1 Schematic drawing of the excimer laser machine system

is much deeper than that of UV lasers. This leads to drilling rates of a few tens of microns per pulse. But it causes poor resolution with a little thermal damage to the substrates. The UV Nd:YAG laser delivers light in the wavelength of 355 nm that is highly reactive with the dielectric materials. Holes can be drilled by an UV Nd:YAG laser which produces pulses of radiation with pulse duration about 0.1 to 1 ms. An excimer laser produces pulses of radiation at a wavelength of 308 nm with pulse duration of 20 to 150 ns [20]. A hole with diameter from 10 to 50 μm can be produced. Williams also reported that highly regular holes, in terms of shape and size, can be produced by using this technique with a “lack of thermal effects” [20].

In this study, key parameters of 248 nm excimer laser which influence the results of drilling include laser fluence, shot number and repetition rate. They are realized for better understanding of its process mechanisms. The excimer laser system is schematically illustrated in Fig. 1. The photomask projection method is applied to micromachining microholes. When a laser beam goes through the photomask, the pattern on the mask is transferred onto PI substrate. During the laser ablation process, photomask and substrate are fixed until microholes are produced. The microhole array is fabricated using 248 excimer laser irradiation on the PI substrate by high precise positioning stepper. The fabrication process of a microhole array is carried out using excimer laser ablation. The quality of the drilled microhole such as kerf geometry and debris formation is discussed and characterized.

2 Experimental technique

PI substrate (wafer) is 50 μm thick purchased from Hisn-Tou company in Taiwan. Its mechanical properties are listed in Table 1. PI exhibits excellent mechanical properties such as tensile strength of 180 MPa, elongation of 80% and Young’s modulus of 2.9 GPa. It shows a high tensile strength, high modulus and good elongation. Thus, it can be considered an excellent material for nozzle plate application.

An Exitech 8000 type excimer laser was used in this study. The present experimental setup, mask position and the workstation are schematically illustrated in Fig. 1. This excimer laser system mainly consists of a short-pulse Lambda Physik COMPEX-110 excimer laser source and Aerotech positioning system. The following are the specifications of the excimer laser used: wavelength

248 nm; maximum pulse energy 400 mJ; pulse duration 25 ns; and maximum pulse repetition rate 100 Hz. The focused spot size of the laser beam was $0.25 \times 0.25 \text{ cm}^2$. Both a constant discharge voltage mode and constant pulse energy mode were available during micromachining. The photomask projection method was applied for micromachining after a constant voltage or pulse energy mode had been set up. A set of twin array energy density homogenizers and a projection lens were installed to make the laser beam power profile more uniform (uniformity to within less than $\pm 1.5\%$). The working parameters of the laser machine were pulse number, laser fluence, and pulse repetition rate, ranging from 200 to 600 shots, 0.576 to 1.344 J/cm^2 and 1 to 100 Hz, respectively.

3 Working principle

The laser projection method uses the shots falling in one place through photomask. The laser projection parameters mainly include laser fluence, shot number, and pulse repetition rate. The relationship between these parameters can be expressed as

$$f = \frac{S}{H/V} \quad (1)$$

where f is the laser frequency, S is the laser shot number, H is the dimension of the mask pattern in the scanning direction (μm), and V is the workstation scanning velocity (mm/min).

As it can be seen from the above expression, although there are many laser variables, i.e. V , S , and f , only two of them are independent. Equation 1 can be rearranged as

$$H = \frac{SV}{f} \quad (2)$$

Equation 2 reveals that H is proportional to S . When a larger H is exposed to the laser beam energy, a deeper workpiece ablation thickness will be achieved. Based on the above mentioned theory, different mask patterns can be designed to obtain various values of H . The laser energy profile in the mask pattern in terms of the laser shot number (see Eq. 2) can be calculated, with which a 3D microstructure can be analogously predicted, such that

$$D \propto KS \quad (3)$$

where D is the ablation depth in the substrate (mm), and K is the coefficient of thermal and photochemical properties.

However, the substrate thermal and photochemical properties were difficult to evaluate. These will play an important role in laser ablation. Thus, the depth is a function of S and K , where K can be treated as a calibration number and is a function of the material thermal and photochemical properties.

Table 1 PI properties

Mechanical	Material PI
Tensile strength	180 MPa
Elongation	80%
Young’s modulus	2.9GPa

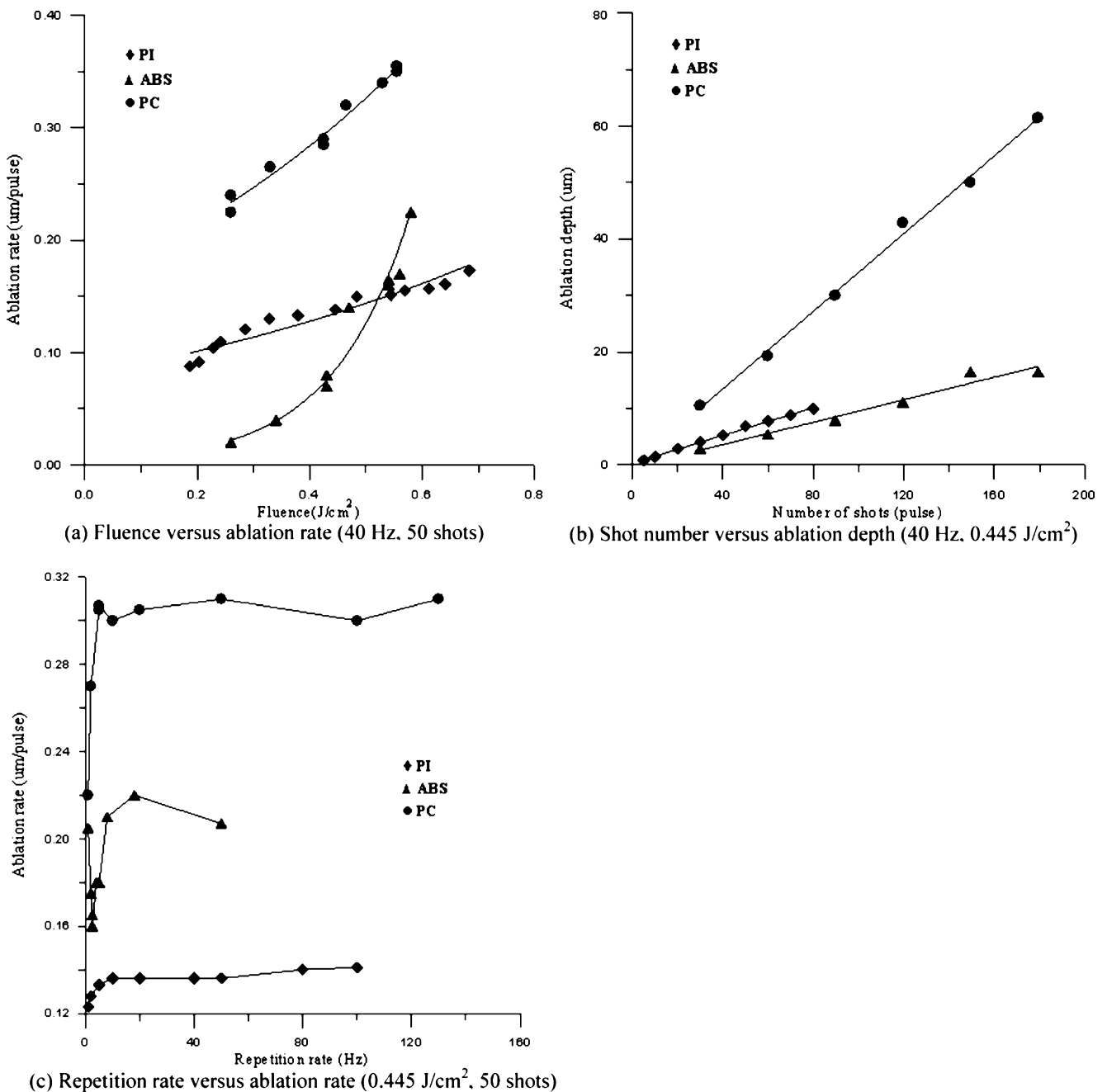


Fig. 2 Process of polymers with excimer laser ablation. **a** Fluence versus ablation rate (40 Hz, 50 shots). **b** Shot number versus ablation depth (40 Hz, 0.445 J/cm^2). **c** Repetition rate versus ablation rate (0.445 J/cm^2 , 50 shots)

Based on Eqs. 2 and 3, as long as the mask pattern is defined, the microhole array produced using laser ablation can be predicted.

In the present laser ablation processing, the PI substrate was used as the workpiece. A laser projection method with various values of laser fluence, repetition rate and shot number was applied to fabricate microholes. The surface of the PI substrate was irradiated with 200 to 600 laser shots at different frequencies and under different fluences in order to ablate a hole in PI substrate. The laser ablated holes' array was subsequently examined using scanning electron

microscopy (SEM) to characterize the 3D morphology. The diameters of the front and back sides were measured and discussed.

4 Results and discussions

The present experiment is conducted based on the laser shot number, energy fluence, and pulse repetition rate. Therefore, the relationship between the mentioned above parameters and the ablation rate was investigated and

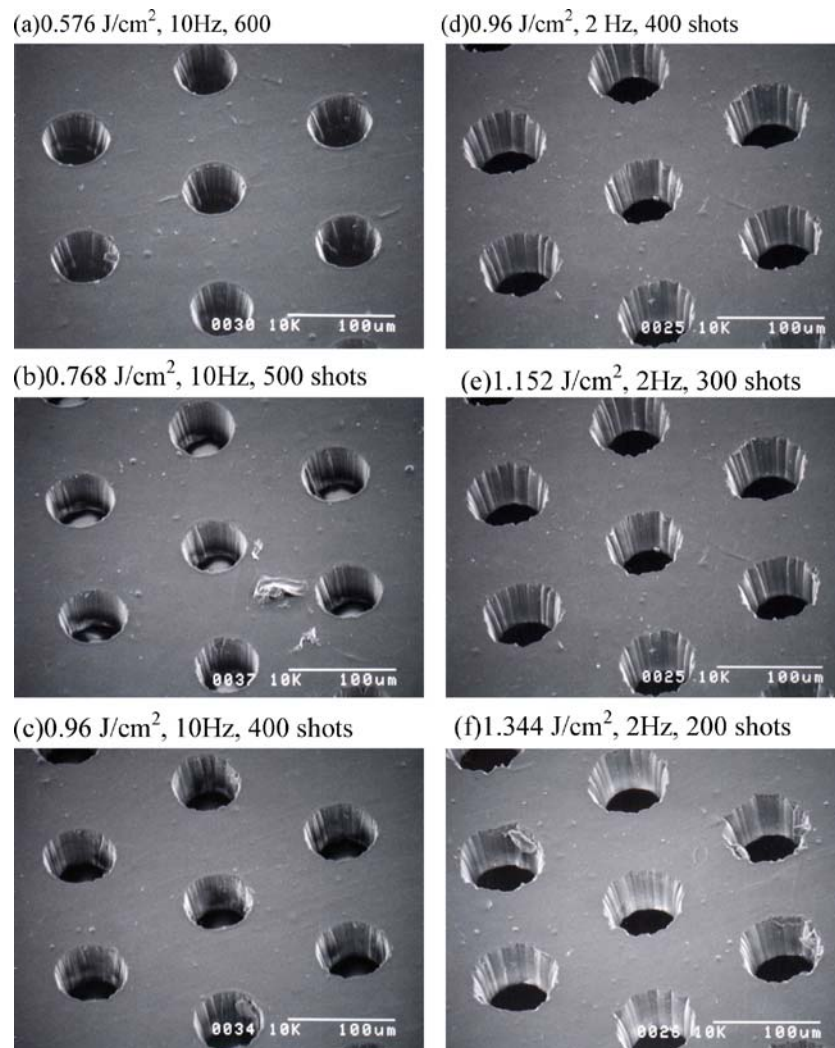


Fig. 3 Comparison between experiments with given values of laser fluence for PI material. **a** 0.576 J/cm², 10 Hz, 600. **b** 0.768 J/cm², 10 Hz, 500. **c** 0.96 J/cm², 10 Hz, 400 shots. **d** 0.96 J/cm², 2 Hz, 400 shots. **e** 1.152 J/cm², 2 Hz, 300 shots. **f** 1.344 J/cm², 2 Hz, 200 shots

characterized. Excimer laser ablation of polymeric materials is tested. Figure 2a shows the ablation rate (depth per pulse; $\mu\text{m}/\text{pulse}$) versus fluence, and Fig. 2b depicts the ablation depth (μm) versus laser shot number. It makes sense that a higher laser energy impinging on material results in higher ablation rate. Figure 2c shows the effect of laser repetition rate. It shows a constant ablation rate per laser pulse at frequencies >10 Hz. It is worth noticing that when frequencies >10 Hz are applied, constant ablation rate per second is achieved. This is due to laser induced plasma preventing the incident laser from the material surface.

Laser pulse energy higher than 200 mJ (per pulse) will destroy Cr film on the conventional quartz photomask significantly during excimer laser projection ablation. Furthermore, a higher pulse energy and repetition rate (>40 Hz) cause cumulative heat in PI substrate.

50 μm thick PI holes are drilled through. Experimental results of the ablated microhole arrays are illustrated in Fig. 3. The laser fluence ranges from 0.576 to 1.344 J/cm²,

shot number is from 200 to 600 shots, and repetition rate is from 2 to 10 Hz. After laser ablation PI, the front and back side diameters of the microhole with a conical shape are observed as shown schematically in Fig. 4.

SEM micrograph in Fig. 5 shows top views of such holes with and without a protecting layer. The PI workpieces are ablated at fluence of 0.576 J/cm² and 1.344 J/

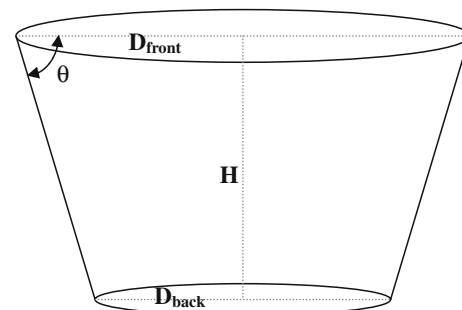


Fig. 4 Diameters of the front and back sides and the taper angle, D_{front} , D_{back} and θ , respectively

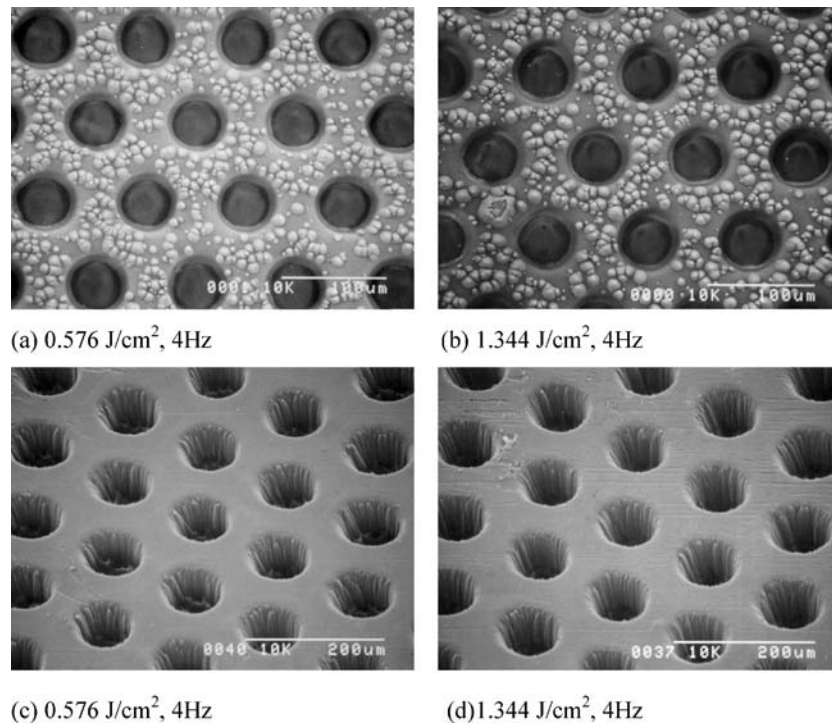


Fig. 5 Comparison between experiments with given values of laser fluence for PI material, shot number 600. **a** 0.576 J/cm², 4 Hz. **b** 1.344 J/cm², 4 Hz. **c** 0.576 J/cm², 4 Hz. **d** 1.344 J/cm², 4 Hz

cm² and at a shot number of 600 and 200, respectively. The differences between the two kinds of ablation conditions can be clearly seen. When PI is without a protective layer, a serious debris formation is deposited on the PI surface as shown in Fig. 5a and b, even after DI water cleaning. It shows that the debris formation increases with the fluence. On the other hand, before the laser process, PI is coated with a protective thin film. When the laser ablation process is finished, chemical solution is used to wash away the coated film. The debris is also washed away. Thus, no debris deposition is observed in the PI surface as shown in Fig. 5c and d. It demonstrates that this method can solve the debris problem on the PI surface effectively.

The ablated diameter of the front and back sides for different laser fluences is realized. The relationship between diameter and fluence is shown in Fig. 6. For fluence

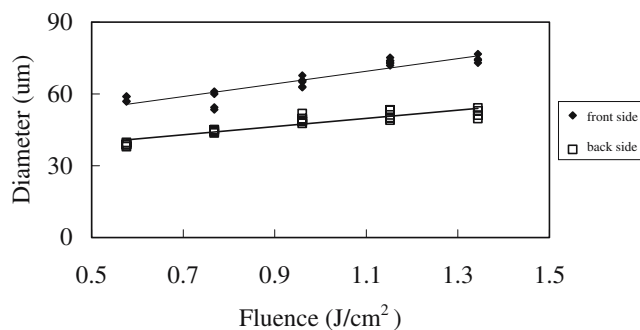


Fig. 6 Dependence of the ablation diameter of the front and back sides on different laser fluences (5 Hz)

0.576 J/cm², for example, the ablated front and back diameters were observed to be 57 μm and 38 μm, respectively. Hence, a conical shape is created in the kerf. The laser beam impinges on the PI substrate. Firstly, the incident energy is absorbed in the front side during the ablation process; then, the energy is absorbed for material removal. This behaviour is why a conical shape of the holes is created. It makes sense that the larger the fluence is, the larger the diameter is. The original hole dimension on the mask is 50 μm in diameter. When fluence is 1.344 J/cm² as shown in Fig. 6, the front diameter of 70 μm can be observed. From the result, the ablated diameters depend on the laser fluence significantly. The conical angle of the hole at different laser fluences is calculated as shown in Fig. 7. The taper angle from 88 to 83 degrees can be observed. It reveals that although the diameter is influenced significant-

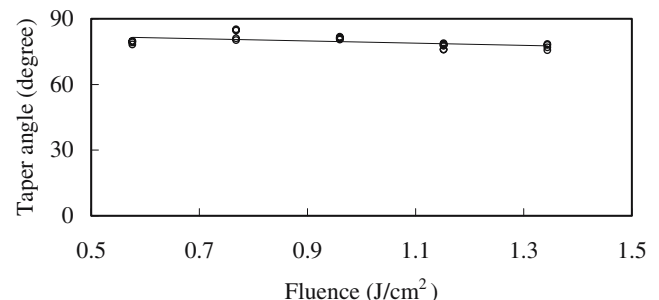


Fig. 7 Dependence of the taper angle on different laser fluence (5 Hz). **a** Repetition rate (Hz) (600 shots). **b** Repetition rate (Hz) (500 shots). **c** Repetition rate (Hz) (800 shots)

ly by laser fluence, the taper angle depends less on that. When a smaller value of laser fluence is applied, a smaller front and back diameter can be observed. On the other hand, when a greater one is applied, it causes an obvious through-hole and leads to a larger front and back side diameter.

Larger front and back side diameters mean that a large portion of the beam energy penetrates down through to the PI substrate. Then a through hole is produced. During the laser drilling experiments, different diameters in the front and back sides of PI substrate can be observed in the ablation process at different laser fluences.

On the other hand, the influence of the repetition rate on the ablated diameter and taper angle is shown in Fig. 8. Extensive experiments on drilling hole with different processing parameters are conducted. SEM micrographs of microholes with different repetition rates from 1 to 10 and different lasers from 0.576 J/cm^2 to 1.344 J/cm^2 are shown in Fig. 9. When more shots or larger fluence are applied, it causes larger diameters in both front and back sides. But compared to fluence, the effect of repetition rate on diameters is not so significant. These results are arranged in matrix form, i.e. process window. Better processing parameters can be easily

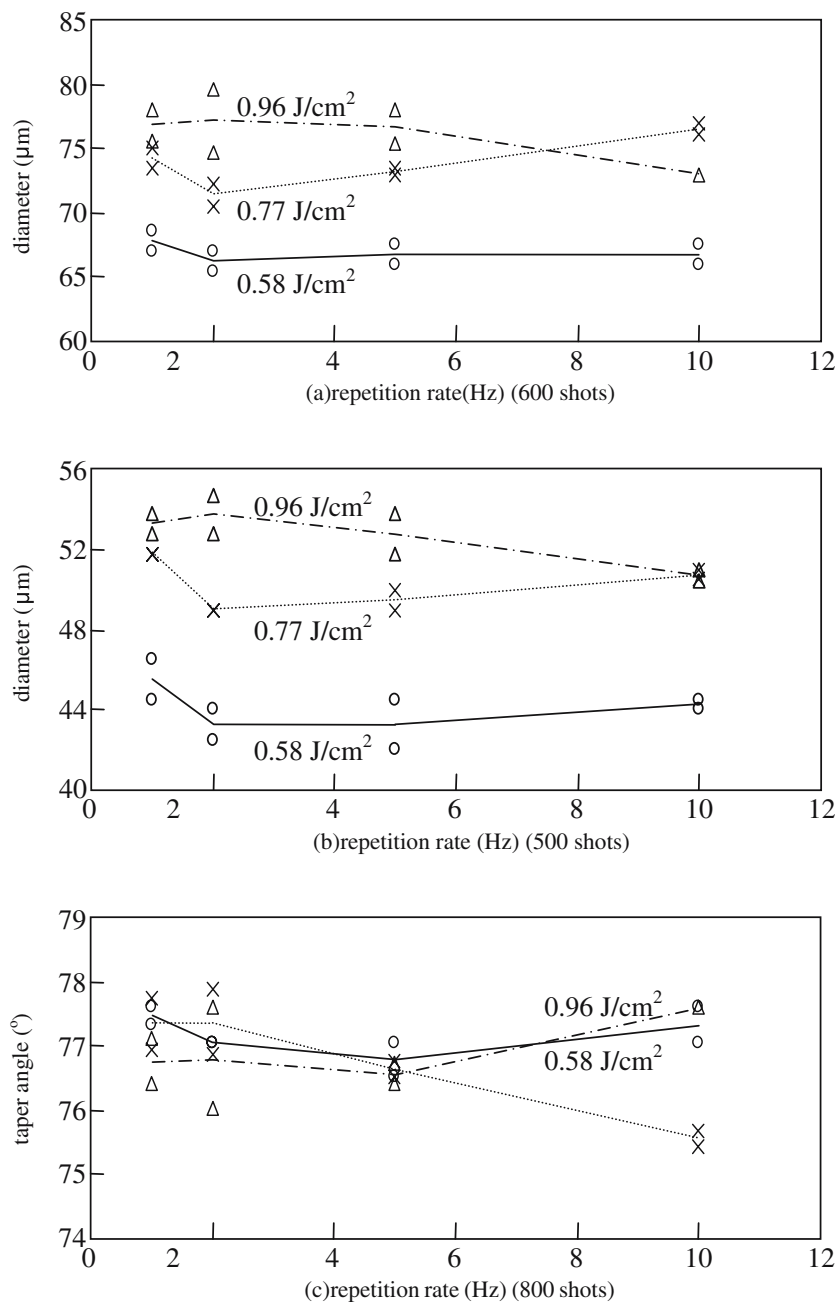
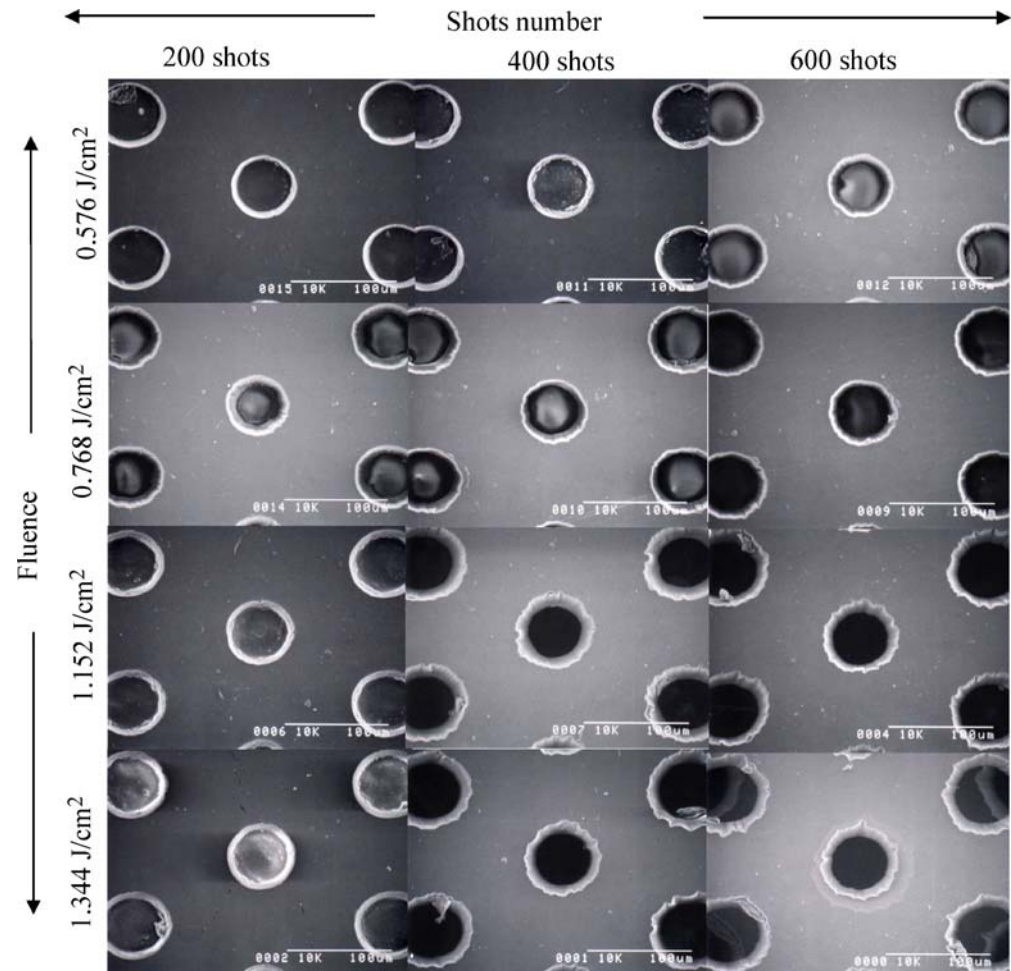


Fig. 8 Influence of the repetition rate on ablation diameter of the front/back sides and taper angle

Fig. 9 SEM images of holes in 50 μm thick PI with protecting layer drilled with different laser fluences and repetition rates at 10 Hz



identified. From the process window, it can be seen that a better ablated quality can be obtained with fluence of 0.768 J/cm^2 . It also reveals that the repetition rate has only a minor influence on the quality of the holes at the front and back sides of the PI, whereas increase in laser fluence leads to an increase in the front and back side diameter.

5 Conclusion

In this study, a micromachining process to fabricate micro-hole arrays using 248 nm excimer laser ablation has been explored. Several sets of experiments were carried out to discuss the process in terms of pulse number, laser fluence, and pulse repetition rate. Various laser fluences from 0.576 to 1.344 J/cm^2 , shot numbers from 200 to 600 and repetition rates from 1 to 10 Hz are realized. The relationships between microhole dimensions and laser processing conditions were studied. Various diameter shapes and sizes can be controlled using different laser beam ablation parameters. Microhole arrays with different diameters on 50 μm thick PI film have been fabricated. The taper angle

from 88 to 82 degree can be observed. It reveals that although the diameter is significantly influenced by laser fluence, the taper angle is less dependent. Besides, to improve the laser machining quality of PI microholes, before excimer laser drilling PI is conducted, the PI surface is pre-coated with and without a thin film material to reduce the formation of debris, respectively. The result shows that the formation of debris can be reduced significantly when a pre-coated thin film is applied on a PI surface.

Acknowledgements The authors would like to thank the Center for Micro/Nano Technology Research, National Cheng Kung University, Tainan, Taiwan, for equipment access and technical support. In addition, financial support from NSC 94-2212-E110-015 as well as NSC94-2622-E-110-017-CC3 is acknowledged.

References

- Hoffmann M, Kopka P, Voges E (1999) Optical fibre switches based on full wafer silicon micromachining. *J Micromech Microeng* 9:151–155
- Momma C, Nolte S, Chichkov B N, Alvensleben F, Tunnermann A (1997) Precise micromachining with femtosecond laser pulses. *Laser Optoelektron* 29(3):82

3. Ashkenasi D, Rosenfeld A, Varel H, Wahmer M, Campbell EEB (1997) Laser processing of sapphire with picosecond and sub-picosecond pulses. *Appl Surf Sci* 120:65–80
4. Kruger J, Kautek W, Lenzer M, Sartania S, Spielmann C, Krausz F (1998) Laser micromachining of barium aluminum borosilicate glass with pulse durations between 20fs and 3ps. *Appl Surface Sci* 127–129:892–898
5. Ameer-Beg S, Perrie W, Rathbone S, Wright J, Weaver W, Champoux H (1999) Femtosecond laser microstructuring of materials. *Appl Surf Sci* 127–129:875
6. Bednarczyk S, Bechir R, Baclet P (1999) Laser micro-machining of small objects for high-energy laser experiments. *Appl Phys A-Mater* 69:S495–S500
7. Simon P, Ihlemann J (1996) Machining of submicron structures on metals and semiconductors by ultrashort UV-laser pulses. *Appl Phys A* 63:505
8. Ihlemann J, Wolf-Rottke B (1996) Excimer laser micro machining of inorganic dielectrics. *Appl Surf Sci* 106:282–286
9. Zergioti I, Mailis S, Vainos NA, Fotakis C, Chen S, Grigoropoulos CP (1998) Microdeposition of metals by femtosecond excimer laser. *Appl Surf Sci* 127–129:601–605
10. Leidinger D, Penz A, Schuocker D (1995) Improved manufacturing processes with high power lasers. *Infrared Phys Technol* 36:251–266
11. Rabello MS, White JR (1997) Crystallization and melting behaviour of photodegraded polypropylene: I. *Chemi-Crystallization*, *Polymer* 38:6379–6387
12. Bauerle D (1996) *Laser processing and chemistry*. Springer, Berlin Heidelberg New York, pp 191–207
13. Rubahn HG (1999) *Laser applications in surface science and technology*. Wiley, New York
14. Srinivasan R (1993) *Appl Phys A* 56A:417–423
15. Zhang Y, Lowe RM, Harvey E, Hannaford P, Endo A (2002) High aspect-ratio micromachining of polymers with an ultrafast laser. *Appl Surf Sci* 186:345–351
16. Gunji M, Nakanishi H, Washizu M (2005) Local in-situ hydrophilic treatment of micro-channels using surface discharge. 2005 international conference on solid state sensors, actuators and microsystems, Seoul, South Korea, pp 1187–1190
17. Oki A, Ogawa H, Nagai M, Shinbashi S, Takai M, Yokogawa A, Horiike Y (2004) Development of healthcare chips checking life-style-related diseases. *Mater Sci Eng* 24 (6–8):837–843
18. Furuess RJ, Tsao TC, Rankin JS, Muth MJ, Manes KW (1999) Torque control for a form tool drilling operation. *IEEE Trans Control Syst Technol* 7:22–30
19. Dupont A, Caminat P, Bournot P, Gauchon JP (1995) Enhancement of material ablation using 248, 308, 532, 1064 nm laser pulse with a water film on the treated surface. *Appl Phys* 78:2022–2028
20. Williams SW, Marsden PJ (1996) New laser drilling techniques for porous surfaces. Second European forum on laminar flow technology, Bordeaux, France, June 1996